The Thermal Chemistry of 1-Chloro-3-Iodopropane (ClC_3H_6I) Adsorbed on Pt(111)

T. B. Scoggins and J. M. White*

Center for Materials Chemistry, Department of Chemistry and Biochemistry, University of Texas at Austin, Austin, Texas 78712

Received: June 11, 1999; In Final Form: September 9, 1999

HREELS and XPS indicate negligible dissociation of ClC_3H_6I during adsorption at 100 K. During TPD, no ClC_3H_6I desorbs for coverages below 0.4 ML. For higher, but not multilayer coverages, parent ClC_3H_6I desorption occurs in two peaks, 200 and 230 K. After even larger doses, unsaturable multilayer desorption occurs at 170 K. HREELS indicates that most C−I bonds dissociate by 205 K. The following reaction paths are proposed on the basis of TPD and HREELS results. When the C−I bond breaks, 3-chloropropyl fragments, $C_{(a)}H_2CH_2CH_2Cl$, are formed and these either lose HCl to form η^3- or η^1-allyl or lose a β-hydrogen to form 3-chloro-di-σ-propylene. Some η^3-allyl groups hydrogenate to either propylene, some of which desorbs at 240 K, or *n*-propyl, some of which hydrogenates to release propane at 250 K. Other η^3-allyl groups isomerize to η^1-allyl. At 250 K, 3-chloro-di-σ-propylene eliminates chlorine as HCl and also releases H atoms that hydrogenate neighboring C_3 fragments. The η^1-allyl fragment either hydrogenates and desorbs as propylene at 325 K or isomerizes to propylidyne. Propyl and di-σ-propylene moieties rearrange to form propylidyne or release propylene at 325 K. Interestingly, there is some benzene desorbing at 375 K. To account for it, a diene metallacycle is suggested. Atomic iodine desorbs at 825 K. Comparisons of the thermal chemistry of ClC_3H_6I on Ag(111) and Ni(100) are made as are comparisons of ClC_3H_6I with other C_3 adsorbates on Pt-(111).

1. Introduction

This paper describes the thermally activated surface chemistry of 1-chloro-3-iodopropane, ClC_3H_6I, on Pt(111). The work is related to companion studies on other C_3 adsorbates investigated in our laboratory, including cyclopropane, c-C_3H_6.[1] We have used electron irradiation of adsorbed c-C_3H_6 at 100 K to synthesize C_3 fragments and have evidence for C_3H_6 metallacycles based on vibrational spectroscopy and surface reaction processes. A trimethylene species, metallacyclobutane or metallacyclopentane, is widely proposed to account for both hydrogenation and hydrogenolysis products from reactions of cyclopropane over supported metal catalysts.[2−18] ClC_3H_6I was chosen for study since it provides an alternative route to C_3 intermediates with potential for forming cyclic intermediates and possesses distinguishable halogens.

In related work on dihalogenated C_3 adsorbates, Bent and co-workers[19] examined 1,3-diiodopropane, 1,3-dibromopropane, and 1,3-dibromopropane-d_6 on Al(100). In all cases, propylene was the major temperature programmed desorption (TPD) product and there was high-resolution electron energy loss spectroscopy (HREELS) evidence for a C_3 metallacycle, $C_{(a)}H_2CH_2C_{(a)}H_2$.[20] Zhou and White[21] studied ClC_3H_6I on Ag(111), dosed at 100 K. During TPD, both C−X bonds break and the intermediate, described as a C_3 metallacycle, rearranges to cyclopropane which desorbs between 210 and 255 K.

In a closely related study, Tjandra and Zaera[22,23] examined the thermal chemistry of both 1,3-diiodopropane, IC_3H_6I, and ClC_3H_6I on Ni(100). In the case of IC_3H_6I, the TPD products were propane, cyclopropane, propylene, and H_2. For ClC_3H_6I, the cyclopropane and propylene desorption peaks are ∼50 K higher than for the diiodo compound, presumably due to the relatively stronger C−Cl bond, and no propane desorbs unless H atoms are coadsorbed. Coadsorption with D leads to propane-d_2 desorption.

Cyclopropane adsorbed on Pt(111) is thermally stable but dissociates under electron irradiation.[1] Postirradiation TPD products are propylene, hydrogen, methane, and ethylene, the latter two products being unique for the C_3 adsorbates we have examined. An η^3-allyl intermediate is identified by HREELS and is responsible for propylene desorption at 208 K. The proposed reaction mechanism includes transient formation of metallacyclopentane and a more stable metallocyclobutane from which methane and ethylene arise. Thermal decomposition of another C_3 precursor, allyl bromide, on Pt(111)[24] forms both η^3-allyl and η^1-allyl (propenyl) groups. Depending on coverage, some η^3-allyl hydrogenates to propylene at 225 K, but most of it decomposes to H_2 and adsorbed C. Thermal decomposition of 1-iodopropane on Pt(111)[25] leads to *n*-propyl groups which undergo either β-hydride elimination to desorb propylene or hydrogenation to desorb propane.

In this paper, we describe the thermal chemistry of ClC_3H_6I on Pt(111) and compare the results with those other found for C_3 precursors and substrates.

2. Experimental

Experiments were performed in an ultrahigh vacuum chamber equipped with HREELS, X-ray photoelectron spectroscopy (XPS), and TPD. The temperature ramp rate for TPD was typically 3 K s^{-1}. The temperature was monitored by a chromel−alumel thermocouple spot-welded to the back of the crystal. The Pt(111) crystal was cleaned, as verified by XPS, by one or both of two procedures: (1) sputtering with Ar^+ ions and annealing at 800 K for at least 5 min, and/or (2) oxidizing in 5×10^{-8} Torr O_2 at 800 K. For both, the substrate was subsequently flashed to >1100 K to remove residual oxygen.

10.1021/jp991923n CCC: $18.00
Published on Web 10/08/1999

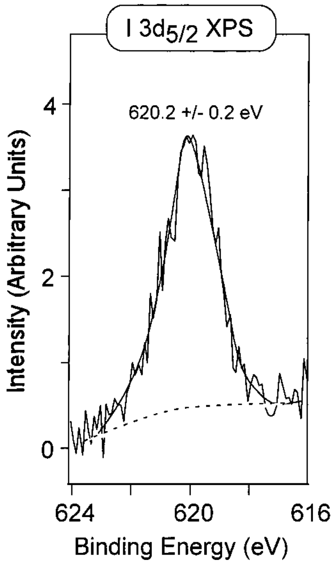

Figure 1. $I(3d_{5/2})$ XPS for 0.5 ML (1.6×10^{14} cm^{-2}) of ClC_3H_6I dosed on Pt(111) at 100 K.

1-Chloro-3-iodopropane, ClC_3H_6I, (99% Aldrich) was further purified by several freeze−pump−thaw cycles. The molecule was dosed by establishing a constant pressure behind a calibrated ca. 10 μm diameter pinhole doser that was reproducibly placed ∼5 mm from the surface using a linear motion device. The pressure behind the pinhole was measured by a MKS absolute pressure transducer and was typically 0.1 Torr. In previous work on C_3H_7I, this doser was calibrated to deliver 1.4 (± 0.15) × 10^{13} C_3H_7I cm^{-2} s^{-1} Torr $^{-1}$.[25] The flux calibration involved XPS measurements of C(1s) and I(3d) intensities for two standards, CO and atomic I, adsorbed at known absolute coverages of CO per surface Pt atom and I per surface Pt atom.[5,11,26] Adjusting for the molecular weight change, the doser will deliver 1.28×10^{13} ClC_3H_6I cm^{-2} s^{-1} Torr^{-1}. For 0.1 Torr, the flux is 1.28×10^{12} ClC_3H_6I cm^{-2} s^{-1} at the Pt(111) substrate.

HREELS measurements employed a primary beam of 1 or 3 eV and a resolution between 65 and 80 cm^{-1} full width at half-maximum (fwhm). All HREELS spectra were recorded at 100−110 K and were normalized to the elastic peak. Vibrational mode positions are assigned as the center of a peak or, in the case of shoulders, the inflection point. The HREELS peak positions are generally determined to within ±10 cm^{-1}.

XPS was done using a standard Mg Kα anode source and 50 eV pass energy. The Pt(4f) line at 70.9 eV was used as an internal reference.

3. Results

3.1. XPS. Figure 1 shows the $I(3d_{5/2})$ XPS peak for an exposure of 1.6×10^{14} ClC_3H_6I cm^{-2} on Pt(111) at 100 K. For this dose, shown below to be 0.5 monolayers (0.5 ML), there is one peak at 620.2 ± 0.2 eV, consistent with nondissociative adsorption, i.e., retaining the C−I bond and forming little if any atomic iodine on Pt(111). Reported $I(3d_{5/2})$ binding energies on Pt(111) are 619.4 ± 0.2 eV[27,28] for atomic iodine compared to 620.4 eV for monolayer CH_3I,[29] 620.2 eV for C_2H_5I[27] and C_3H_7I,[25] and 619.9 eV for C_2H_3I on Pt(111).[28] This observation demonstrates that nondissociative adsorption of ClC_3H_6I dominates on Pt(111) at 100 K for 0.5 ML, and presumably at all coverages used here, i.e., ≥0.1 ML. Nondissociative adsorption is consistent with the HREELS data presented below.

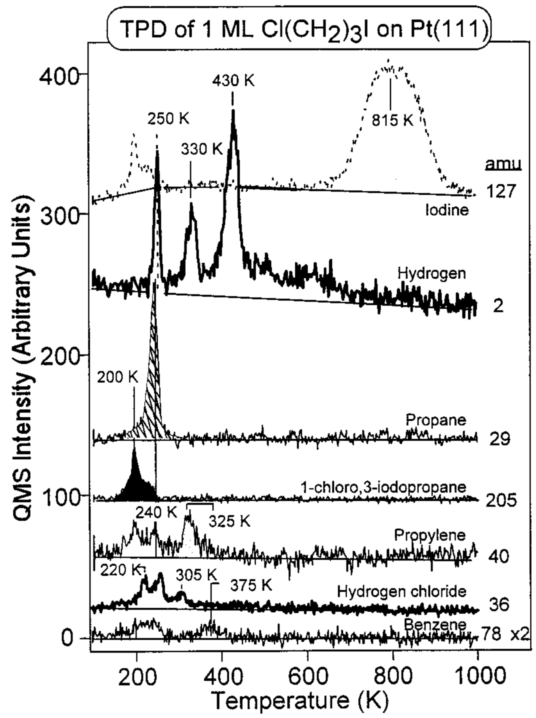

Figure 2. Product desorption (TPD) from 1 ML of ClC_3H_6I dosed on Pt(111) at 100 K. Products (mass of fragment followed), from top to bottom, are atomic iodine (127 amu), dihydrogen (2 amu), propane (29 amu), 1-chloro-3-iodopropane (205 amu), propylene (40 amu), hydrogen chloride (36 amu), and benzene (78 amu).

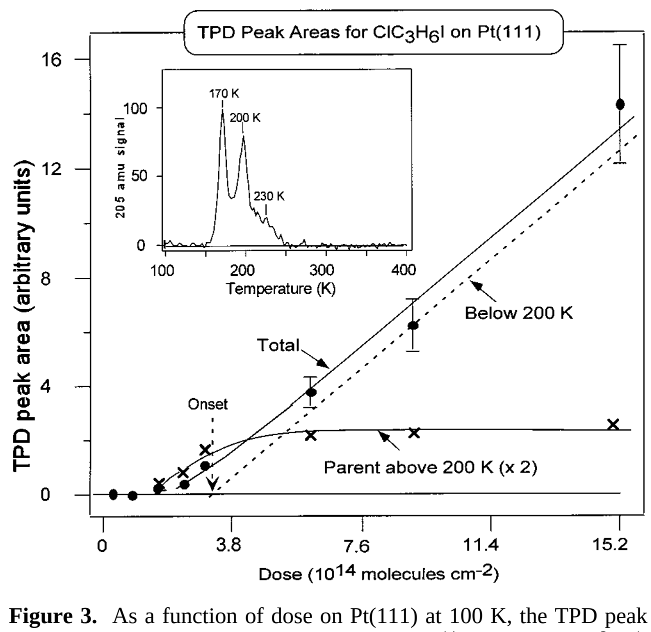

Figure 3. As a function of dose on Pt(111) at 100 K, the TPD peak area of parent ClC_3H_6I. For a dose of 3.8×10^{14} molecules cm^{-2} s^{-1}, the inset shows TPD the profile for multilayer with unsaturable peak at 170 K and monolayer peaks at 200 and 230 K. The dashed curve is the difference between the total peak area (filled circles) and the monolayer peaks (×). The dose rate was 1.28×10^{14} molecules cm^{-2} s^{-1}.

3.2. TPD. Extensive dosing leads to an unsaturable multilayer ClC_3H_6I peak at 170 K (Figure 3). For a monolayer (ML) dose, defined below, the TPD, Figure 2, exhibits clear evidence for ClC_3H_6I desorption and for thermally activated bond breaking leading to desorption of six products: H_2, C_3H_6, C_3H_8, HCl, C_6H_6, and I. There was no evidence for other desorbing products. In particular, there was no evidence for cyclopropane, c-C_3H_6, desorption based on fragmentation patterns in the 40−42 amu region.[23]

Parent desorption (205 amu) is relatively broad with peaks at 200 and 230 K (darkened areas). Ion source fragmentation of the parent is clear in the 127, 78, and 40 amu traces. As expected, atomic iodine desorption (127 amu) is broad and peaks at 825 K. Hydrogen desorption (2 amu) exhibits three peaks, 250, 330, and 430 K, and shows broad low intensity desorption out to 750 K. The H_2 desorption profile, for $T \geq 300$ K, follows qualitatively, but not quantitatively, that observed for the thermal decomposition of propylidyne fragments formed from either propylene or allyl species on Pt(111).[24] The sharp H_2 peak at 250 K is unique among the C_3 adsorbates we have studied.

There are C_3 species desorbing with peaks at 240 ± 10 and 325 ± 5 K. These are assigned to propane and propylene. The 29 amu signal is strong for propane (hatched area) while 40 amu is very weak. The reverse holds for propylene (gray area). Thus, propane and propylene both desorb at 240 K, while propylene dominates at 325 K. The 40 amu peak at 240 K, while dominated by propylene, does contain some parent ClC_3H_6I fragmentation contribution. The formation of propane, C_3H_8, requires hydrogenation, and it is intuitively satisfying that the 240 K propane peak overlaps strongly with desorption of H_2 which peaks at 250 K.

Unlike iodine that desorbs atomically between 700 and 900 K, chlorine is eliminated from the surface as HCl (36 amu) in three peaks: 220, 250 and 305 K. Among the C_3 adsorbates we have examined, desorption at low temperatures of a hydrogen halide is a second unique feature of ClC_3H_6I on Pt(111). A third unique feature of ClC_3H_6I is the small, reproducible desorption of a 78 amu product at 375 K. There is also a 78 amu signal between 200 and 260 K which cannot be entirely attributed to ClC_3H_6I. These peaks are assigned to benzene; the fragmentation pattern for benzene is dominated by 78 amu ($C_6H_6^+$) with no other ions contributing more than 20% of the 78 amu peak.

The *sequence* of desorbing products is noteworthy. Using Figure 2, the first reaction product desorbing is HCl at 220 K. This is followed at 240 K by a mixture of C_3H_8 and C_3H_6 and about 10 K higher by a large H_2 desorption. No more than 5−10 K higher, there is a second HCl peak. As described above, some benzene desorbs in this region. This flurry is followed by little desorption activity up to 300 K where another burst of HCl (305 K) desorbs, followed by H_2 and C_3H_6, but no C_3H_8, at 325 K. Above 400 K, there is a large H_2 peak at 430 K with a long tail out to 750 K and finally a broad atomic I desorption between 700 and 900 K. We return to this sequence in the discussion section where it is used to constrain the plausible reaction paths.

As indicated in Figure 3, low doses of ClC_3H_6I dissociate while extensive doses exhibit three ClC_3H_6I TPD peaks at 170, 200, and 230 K (inset of Figure 3). There is some growth of the 200 K peak after the 170 K peak begins to appear, likely the result of some islanding and growth of second and higher layers before the first layer is everywhere completed. Above 6.4×10^{14} cm^{-2} in Figure 3, the dashed line is the difference between the total ClC_3H_6I desorption and that involved in the two higher temperature peaks, i.e., a measure of the amount of ClC_3H_6I adsorbed into the multilayer. Extrapolation indicates an onset close to 240 s (3.1×10^{14} ClC_3H_6I cm^{-2}). This dose equals, within experimental error, the number density, ClC_3H_6I cm^{-2}, estimated from the liquid-phase density, ρ. The density (1.90 g cm^{-3}) corresponds to 3.2×10^{14} ClC_3H_6I cm^{-2}. On this basis, we can reasonably conclude an absolute monolayer coverage of 3.1 (± 0.4) $\times 10^{14}$ ClC_3H_6I cm^{-2} and a sticking coefficient close to unity. Thus, 1 ML ClC_3H_6I corresponds to 0.2 ClC_3H_6I per surface Pt atom.

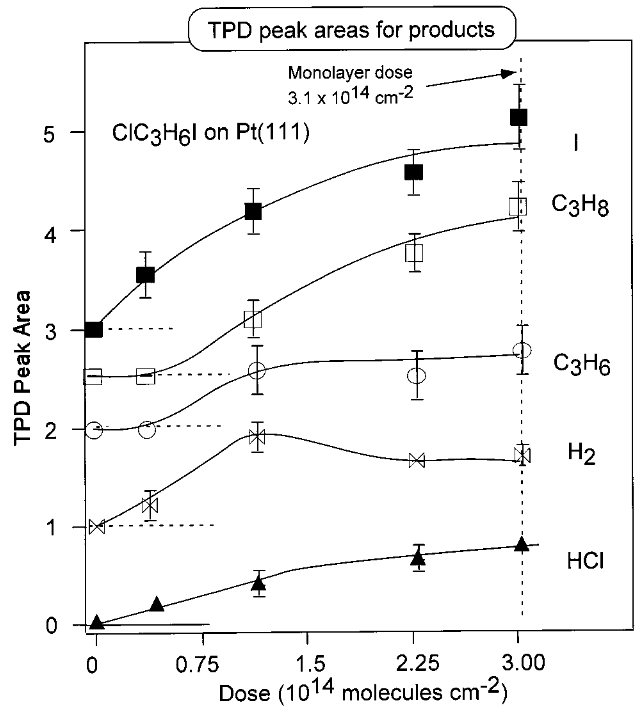

Figure 4. As a function of ClC_3H_6I dose up to 1 ML (3.1×10^{14} molecules cm^{-2} s^{-1}), TPD peak areas for desorbing products. For clarity, zeros for each curve are offset as indicated.

Thermal desorption peak areas for the observed products versus submonolayer dose (Figure 4) indicate that, for a dose of 0.38×10^{14} cm^{-2}, the only products found in TPD are I, HCl, and H_2. This corresponds to a coverage of 0.12 ML of ClC_3H_6I and requires an H/Cl ratio of 6 in the HCl and H_2 desorbing. Consistent with the behavior of fragments derived from other C_3 adsorbates,[24,1,25] all the C remains up to the maximum TPD temperature of 1000 K. For higher doses, a shortage of open Pt sites limits decomposition and, thus, other reaction channels become competitive, e.g., the formation and desorption of propane and propylene. Up to $\sim 1.2 \times 10^{14}$ cm^{-2} (∼0.4 ML), little, if any, ClC_3H_6I desorbs (Figure 3), but as the dose increases further, parent desorption becomes competitive in locales where all the Pt sites are occupied either with dissociation products or undissociated ClC_3H_6I. H_2 and C_3H_6 do not increase above 0.4 ML; in fact, the H_2 peak area drops measurably, a point which we take up below. C_3H_8 and I continue to rise up to 3.1×10^{14} cm^{-2} (1 ML) but are saturated for longer doses (not shown). HCl rises steadily and saturates at 1 ML.

It is noteworthy that the only Cl-containing TPD products are HCl and ClC_3H_6I. Further, as for other C_3 hydrocarbons,[1,24,25] except electron irradiated c-C_3H_6,[1] there is no detectable C_1 or C_2 hydrocarbon desorption. The formation and desorption of 1-chloropropane, C_3H_7Cl, does not contribute.

As a function of dose time, the reaction product thermal profiles are, with a few exceptions, like those shown in Figure 2. The noteworthy exceptions are (1) for a 0.38×10^{14} cm^{-2} dose, there is neither propane nor propylene desorption and the 250 K H_2 peak is absent, and (2) the number of HCl peaks varies with dose—one peak (250 K) up to 0.4 ML, 2 peaks (250 and 300 K) for a 0.75 ML dose, and three peaks (220, 250, and 305 K) for a ML dose. These changes are all attributable to variations of Pt sites with local coverage.

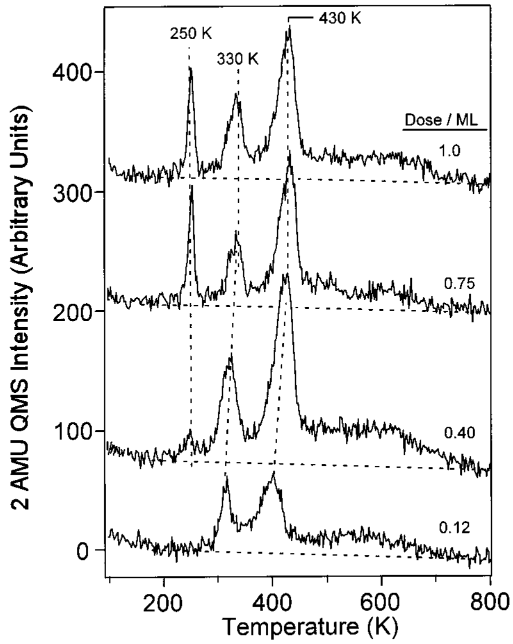

Figure 5. H_2 desorption as a function of ClC_3H_6I dose.

The H_2 TPD profiles, Figure 5, indicate a path change in part of the dehydrogenation when the coverage exceeds 0.4 ML; that is, the strong and narrow H_2 peak at 250 K is barely evident for a dose of 0.4 ML but is saturated for a dose of 0.75 ML. The increasing area of this peak is more than offset by a nearly uniform H_2 intensity decrease above 300 K. Although not examined in detail, benzene desorption begins in the same dose interval.

3.3. HREELS. *HREELS at 100 K.* HREELS was undertaken to characterize intermediate C_3 species formed by thermal activation of two different ClC_3H_6I doses—near monolayer (1.2 ML) and multilayer (3 ML), Figure 6. Since XPS and TPD results show clearly that multilayers formed at 100 K are not dissociated, spectrum 6a can be used as an HREELS "fingerprint" for this adsorbate. For a monolayer dose, XPS evidence indicates negligible C−I bond breaking, so spectrum 6b can be interpreted as molecular ClC_3H_6I interacting with Pt(111). Assignments and comparisons are listed in Table 1. Only vibrational data for other dihalopropanes (liquid) is included since no gas- or liquid-phase ClC_3H_6I data could be located. As expected, modes associated with the CH_2 groups and with the C−Cl and C−I stretches are readily identified. There are no significant changes in loss energies between the two spectra in Figure 6, indicating that interactions between Pt and ClC_3H_6I do not alter measurably the curvatures of the intramolecular potential energy surface that determine the vibrational frequencies.

There are, however, changes in the intensity distribution. The C−H stretch (2970 ± 10 cm^{-1}) and CH_2 scissor modes (1420 ± 5 cm^{-1}) are of about equal intensity in both spectra, but when the C−H stretching regions are normalized to each other, there is uniformly higher relative intensity in the low-energy region (<1400 cm^{-1}) for the 1.2 ML case. These modes include the C−I stretch (510 cm^{-1}), the C−Cl stretch (660 cm^{-1}), and several rocking and twisting CH_2 modes (particularly 740 ± 10 cm^{-1}). Relative intensity differences are not surprising since, with respect to the Pt(111) surface, the average orientation of the principal axes of ClC_3H_6I likely differs in the first layer where interactions with the substrate lead to alignment even though the adsorption energy is weak. We expect the weakly held ClC_3H_6I to align, at *monolayer coverage*, with the highly polarizable iodine atom toward the surface and, to minimize crowding, with the major molecular axis tilted away from the surface plane toward the surface normal. At the Pt(111) surface, there will be enhanced dipole excitation of vibrational modes for which alignment increases the average normal component of the associated transition dipole moment.

While the three different methylene groups and the different conformers of ClC_3H_6I each will have slightly different characteristic vibrational frequencies, the HREELS resolution precludes resolving them. In Figure 6, the highest energy vibrational modes, 2970 ± 30 cm^{-1}, are assigned to a superposition of C−H stretching nodes. There are no CH or CH_3 groups in ClC_3H_6I, so the mode at 1430 (±10) cm^{-1} is readily assigned as CH_2 scissoring. The 1300 cm^{-1} peak is assigned to a CH_2 wag. The mode at 1200 cm^{-1} is assigned to a CH_2 twist. There is a mode just above 1100 cm^{-1} assigned to a CH_2 twist; a C−C asymmetric stretch could also contribute. The strong mode at 740 cm^{-1} is assigned as CH_2 rocking. There is also unmarked poorly resolved intensity at ca. 1000 cm^{-1} that is assigned to a symmetric C−C stretch. The mode at 660 cm^{-1} is assigned to the C−Cl stretch, and the 520 ± 10 cm^{-1} peak to the C−I stretch. Finally, there is a peak at 410 cm^{-1} for 1.2 ML ClC_3H_6I which is consistent with a CCC bend. The agreement with other dihalopropanes, Table 1, is quite satisfactory.[30]

HREELS After Annealing. Heating either coverage of ClC_3H_6I of Figure 6 to 235 ± 3 K leads to changes in the HREELS spectra (Figure 7) that reflect bond breaking to form adsorbed fragments, some of which desorb as demonstrated in TPD. According to TPD (Figures 2 and 4), heating to 235 K moves past ClC_3H_6I desorption and includes some HCl evolution. Each curve of Figure 7 involves the following procedure: clean the substrate, dose ClC_3H_6I at 100 K, heat (3 K s^{-1}) from 100 to 235 K, recool, and acquire spectrum. When intensities are normalized at 2970 cm^{-1}, the two spectra of Figure 7 overlap closely above, but not below, 1000 cm^{-1}. Below 800 cm^{-1}, especially at 660 and 520 cm^{-1}, the relative intensities are significantly higher for the 3 ML case. This region comprises C−Cl and C−I stretching modes, and we conclude that, while heating to 235 K removes the ClC_3H_6I and breaks most of the C−I bonds in both cases, significantly more C−Cl bonds remain when annealing 3 ML. As noted below, a CH_2 twisting mode may contribute at 520 cm^{-1}. Between 750 and 1000 cm^{-1}, a region typical of rocking modes of CH_2 (Table 1), the relative intensities are slightly lower for the 3 ML case (gray area). Consistent with the C−Cl stretching region, we take this as reflecting the formation of more ClC_3H_6 groups for the 3 ML case.

Figure 8 illustrates the major changes that occur upon annealing 3 ML ClC_3H_6I from 100 to 190 K and 1 ML from 100 to 205 K. For both cases, the initial HREELS profile is overlain (bold) with normalization at 2970 cm^{-1}. For 3 ML, little of the expected ClC_3H_6I desorption (Figures 2 and 3) has occurred at 190 K, but compared to the initial spectrum, there are enormous changes between 400 and ~1350 cm^{-1} (gray region). At 1420 cm^{-1}, the two spectra are indistinguishable.

For the 1.2 ML case, negligible ClC_3H_6I desorption occurs up to 205 K. Some desorbs between 210 and 240 K (Figure 3). The corresponding HREELS spectra, again normalized at 2970 cm^{-1}, differ in the following respects: (a) the 870 cm^{-1} peak is stronger after annealing; (b) the 760 cm^{-1} peak is stronger before annealing; (c) the region between 1035 and 1440 cm^{-1} is stronger before annealing. These differences are consistent

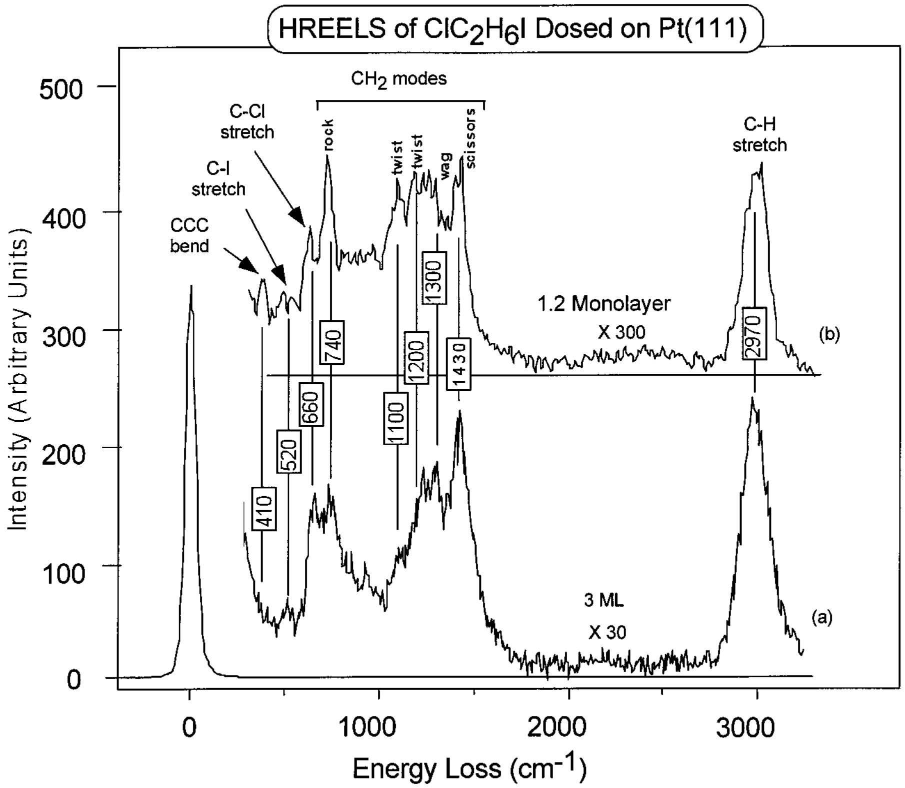

Figure 6. Dosed on Pt(111) at 100 K, HREELS of (a) 3 monolayers and (b) 1.2 monolayers of ClC_3H_6I.

TABLE 1: Vibrational Data of Dihalopropanes and 1-Chloro-3-Iodopropane on Pt(111)

assignment	IC_3H_6I[a]	ClC_3H_6Cl[a]	BrC_3H_6Cl[a]	multilayer ClC_3H_6I[b]	monolayer ClC_3H_6I[b]
C−H str	3004	3001	3000		3000
C−H str	2954	2967	2963	2970	2940
C−H str	2837−2900	2868−2925	2852−2925		
CH_2 scis	1418−1450	1421−1455	1420−1442	1420	1440
CH_2 wag	1275/1342	1270−1357	1243−1355	1300	1300
CH_2 twist	1112/1208	1150/1194	1206/1264		1200
CH_2 twist	1094		1121−1184	1100	1110
asym. C−C str	1072	1077	1076		
sym. C−C str	960	990	978	925	
CH_2 rock	824/914	810/867	859/952	850	
CH_2 rock	732		767/778	740	740
sym. C−X str	530	679	662 C−Cl	660 C−Cl	660
			568 C−Br	510 C−I	525
asym. C−X str	491	641			
CCC bend	398	457	411−443		410
CCX bend	289	354	324−355		
torsion	180	190	245		
torsion	170	180			

[a] All vibrational data for diodopropane, dichloropropane, and bromochloropropane are taken from ref 30. [b] This work.

with the following general model. annealing 1.2 ML to 205 K breaks most of the C−I bonds to form $ClCH_2CH_2C_{(a)}H_2$ which is very unstable and loses HCl at slightly higher temperatures to form $C_{(a)}HC_{(a)}H_2C_{(a)}H_2$, i.e., η^3-allyl. The loss of C−I bonds is accompanied by a reorientation of the major axis of the C_3 species so that the CH_2 rocking mode at 870 cm^{-1} intensifies while that at 740 cm^{-1} weakens. Consistent with an orientation change, other modes dominated by methylene wagging, scissoring, and twisting motions are suppressed with respect to the C−H stretching intensity.

The changes in the 3 ML case are more striking. With respect to the C−H stretching modes centered at 2970 cm^{-1}, the C−I and C−Cl modes intensify and sharpen significantly even though some ClC_3H_6I desorbs. We take this as reflecting orientational changes that lead to a ordering of adsorbed ClC_3H_6I, but little C−I bond breaking. The 740 cm^{-1} CH_2 rocking mode is very strong, while that at 870 cm^{-1} is absent. This is consistent with the above correlation between C−I bond breaking and an intensity shift from 760 to 870 cm^{-1}; that is, upon annealing 3 ML of ClC_3H_6I to 190 K, most of the C−I bonds do not break. The 870 cm^{-1} band is consistent with CH_2 rocking in liquid dichloropropane.[30]

Comparing the spectra of Figures 6−8, we conclude that there are structural rearrangements between 100 and 190 K, between 190 and 205 K, and between 205 and 235 K, each of which has a major impact on at least one of the CH_2 rocking modes. We propose that the surface is dominated by ClC_3H_6I up to 190 K and that there is facile C−I bond breaking between 190 and 205 K to form 3-chloropropyl groups, $C_{(a)}H_2CH_2CH_2Cl$, which react between 205 and 235 K to form di-σ-bonded 3-chloropropylene, $C_{(a)}H_2CH_{(a)}CH_2Cl$, and η^3-allyl, $C_{(a)}H_2C_{(a)}HC_{(a)}H_2$.

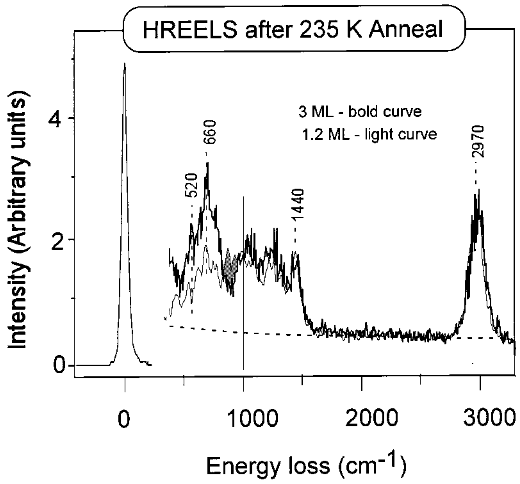

Figure 7. HREELS after annealing 3 ML (bold curve) and 1.2 ML (light curve) of ClC_3H_6I to 235 K. The two spectra are normalized at the peak of the C−H stretch (2970 cm^{-1}). Just below 1000 cm^{-1}, the small intensity excess of the 1.2 ML case is darkened.

Annealing to higher temperatures, selected to correlate with TPD features, furnishes the spectra shown in Figure 9. Between 240 and 270 K, significant amounts of H_2, C_3H_6, C_3H_8, and HCl desorb, and there is a major spectral change in the 660 cm^{-1} region indicating the loss of C−Cl bonds. There is no evidence for a Pt−Cl stretch, supporting a model involving concerted formation of HCl. Otherwise, all the HREELS peaks present at 235 K remain at 270 K with only modest shifts of relative intensities. The modes at 410 and 520 cm^{-1} become better resolved while the C−Cl stretch intensity becomes very weak. Since no C−I bonds remain, the 520 cm^{-1} peak is attributed to CH_2 twisting. There is a now a strong mode at 800 cm^{-1}, and the modes at 1200 and 1440 cm^{-1} sharpen. This spectrum is consistent with the dominant species being η^3-allyl.[24] The 800 cm^{-1} mode is characteristic of methylene rocking in this species. Upon heating to 300 K (not shown), a small amount of HCl desorbs, and the C−Cl mode completely disappears. Otherwise, the HREEL spectrum remains the same as Figure 9b.

The next major change occurs upon heating to 350 K, Figure 9c, which desorbs C_3H_6 and H_2. The vibrational modes in the 800 to 1300 cm^{-1} region weaken, while the C−H stretching region weakens considerably and broadens compared to Figure 9b. Heating further to 450 K desorbs considerable H_2 and some C_6H_6. The HREELS, Figure 9d, is characterized by significantly weaker methylene scissoring intensity (1440 cm^{-1}), relatively stronger and sharper C−H stretching peaking at higher energy (3000 vs 2970 cm^{-1}), and a stronger relative intensity between 800 and 900 cm^{-1}. At this temperature, the H/C ratio is quite low (between 0.5 and 0.7), a common characteristic of the dehydrogenation of C3 species on Pt(111).[31] Thus, we expect few, if any, remaining methylene groups and a distribution of C_xH_y species with $y \leq x$. The distribution of values of x may include 6, since the desorption of benzene requires linkage of six carbons.

4. Discussion

4.1. Overview. To begin a discussion of the thermal chemistry of ClC_3H_6I on Pt(111), we summarize in Scheme 1 proposed reaction paths for monolayer coverage. Variations for higher and lower coverages are discussed in the context of Scheme 1. After providing evidence for the various steps in these paths and plausibility in the absence of evidence, we briefly make comparisons with ClC_3H_6I on Ni(100)[23] and Ag(111)[32] substrates and of ClC_3H_6I with other C_3 adsorbates on Pt(111).

Following Scheme 1, there is, for all coverages, ample XPS and HREELS evidence for little or no dissociative adsorption of 300 K ClC_3H_6I onto 100 K Pt(111). In TPD, the presence of products other than ClC_3H_6I requires thermally activated dissociation and reaction processes. On the basis of the behavior of multilayer TPD, all these dissociative processes occur in the first monolayer. Between 100 and 190 K, there is HREELS evidence for significant restructuring within the adsorbed ClC_3H_6I layer but no HREELS or TPD evidence for dissociation. Consistent with other literature, we suppose for submonolayer coverages, however, that C−I bonds begin to break as low as 160 K. Since the C−Cl bond is stronger than C−I and since the polarizability of I is large, we make two inferences: first, the C−I bond breaks first, and second, for monolayer coverage, the major axis of ClC_3H_6I will be tilted away from the Pt(111) surface plane with the I preferentially next to the Pt. For monolayer and higher coverages, some undissociated ClC_3H_6I desorbs and, between 190 and 205 K, C−I bonds break (B in Scheme 1) as Pt sites become available.

As the temperature increases from 205 to 230 K, the C(a)-$H_2CH_2CH_2Cl$ fragment shown in (B) follows one of two paths; the first forms either η^3-allyl (E in Scheme 1) or η^1-allyl (G in Scheme 1) and the second involves dehydrogenation to form a di-σ-bonded C_3 species that retains a C−Cl bond (D in Scheme 1). Unfortunately, we were unable to identify clearly species D. Along the first path there is TPD of HCl (220 K). The simplest model that captures this result is an intra-adsorbate transition state (C of Scheme 1) that brings the Cl and a methylene H into contact with Pt, a transition requiring locally available vacant Pt sites. Consistent with HREELS, the second path involves retention of C−Cl bonds with significant alteration of methylene vibrational modes. There is no evidence for accumulation of Cl bonded to Pt.

Intramolecular elimination from the chlorinated C_3 species (D) is proposed as the source of the HCl desorption at 250 K (Figure 2). Speculatively, we propose that the H-deficient $C_{(a)}H_2C_{(a)}HC_{(a)}H$ that results from HCl elimination promptly dehydrogenates further to form C_3H_y, $y \leq 3$ (F in Scheme 1). There is competition among several channels for these H atoms. Besides recombination to release H_2, these channels include hydrogenation of η^3-allyl to propyl (J in Scheme 1), likely through a transient $C_{(a)}H_2CH_2C_{(a)}H_2$ species, and propane and hydrogenation of η^3-allyl to di-σ-bonded propylene (H in Scheme 1) and propylene. In passing, note that dechlorination is not complete; the remaining Cl (not shown) is released as HCl with a peak at 305 K (Figure 2).

Between 305 and 330 K, propylidyne (K in Scheme 1) forms either by isomerization of η^1-allyl or by dehydrogenation of di-σ propylene and propyl. The hydrogen either recombines to release H_2 or hydrogenates neighboring η^1-allyl to form and desorb propylene. β-Hydride elimination of propyl may also contribute to the available H bound to Pt and to the desorbing propylene.

For completeness, Scheme 1 must include a path to benzene. While this is an important observation, we can only speculate about the mechanisim and note that acetylene trimerization can form benzene. One plausible path links two η^1-allyl groups, C(a)$H_2CH{=}CH_2$, that with low probability are formed adjacent to each other. This linkage involves forming a metallacycle (L in Scheme 1) that subsequently dehydrogenates either to form and desorb benzene or to contribute to the formation of surface

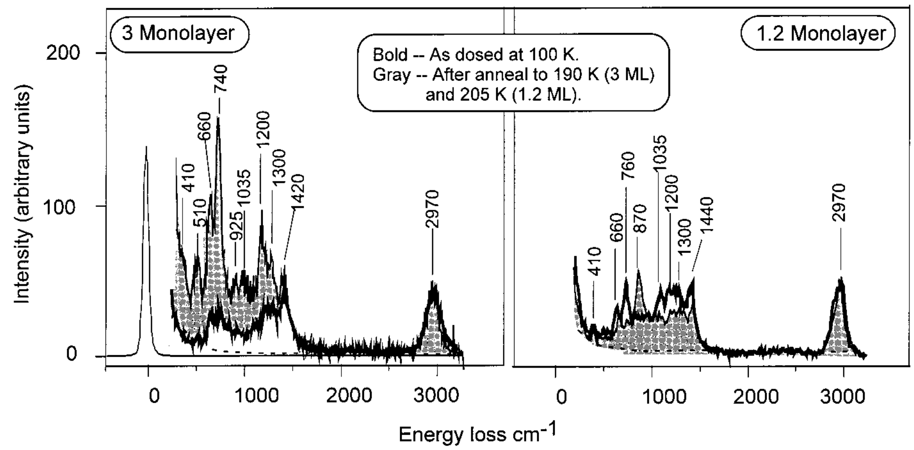

Figure 8. The effects of thermal annealing on HREELS for 3 ML (left side) and 1.2 ML (right side). Spectra are normalized at the C−H stretch (2970 cm^{-1}). Darkened areas emphasize the spectra after annealing to 190 K for the 3 ML case and 205 K for the 1.2 ML case.

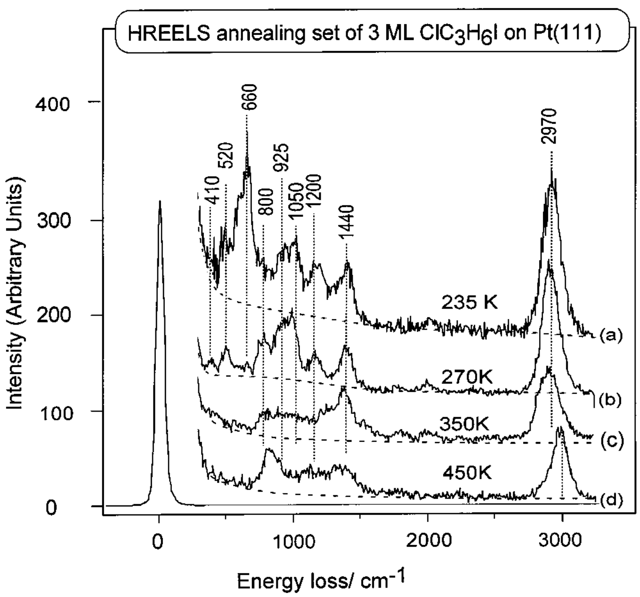

Figure 9. An HREELS annealing set ($T \geq 235$ K) for an initial 3 ML dose of ClC_3H_6I on Pt(111).

carbon. In the presence of $I_{(a)}$ it is also plausible that η^3-allyl moieties are occasionally paired and link to form benzene.

4.2. Comparison: Pt(111), Ag(111), and Ni(100). It is of interest to briefly compare the results reported here with those reported for ClC_3H_6I dosed on Ag(111)[32] and Ni(100).[23] On all three, as generally expected, metal sites of various kinds are available but have limited surface densities. Site availability as a function of temperature and coverage, thus, often constrains thermally activated reaction paths; for example, breaking bonds during heating of molecularly adsorbed species is often inhibited as the initial coverage approaches a monolayer, unless desorption occurs to make sites available.

For ClC_3H_6I adsorbed nondissociatively on all three substrates, thermally activated C-halogen bond breaking occurs readily for submonolayer coverages and temperatures between 160 and 220 K. Thus, for submonolayers, only those halogenated hydrocarbons that desorb below 160 K can escape dissociation. The situation for C−H and C−C bonds is quite different. Ag(111) is typically much less aggressive than either Pt(111) or Ni(100) with respect to breaking C−C and C−H bonds. Consequently, for hydrocarbon fragments and atomic hydrogen adsorbed on Ag(111), C−C and C−H bond formation processes are typically dominant reaction pathways. Indeed, that is the case for adsorbed ClC_3H_6I; the only hydrocarbon reaction product is cyclopropane, c-C_3H_6, that desorbs between 210 and 255 K.[32] At TPD temperatures above 700 K, AgCl and atomic I desorb. These results were accounted for by a reaction path involving breaking the C−I and C−Cl bonds to form atomic I and Cl bound to Ag and a C_3 metallacycle (not characterized) bound to Ag at the first and terminal carbons. Activation of the metallacycle is limited to cyclization, leading to reaction-limited thermal desorption of c-C_3H_6.

The situation on both Ni(100) and Pt(111) is significantly more complex since, if metal sites are available, C−H bonds are activated at relatively low temperatures. At such temperatures, the resulting atomic H is typically active and mobile. Thus, coincident hydrogenation and dehydrogenation is common, some species losing H, others gaining H. This is the situation for ClC_3H_6I on Ni(100)[23] and, as reported here, on Pt(111).

Turning to C−C bonds, under the ultrahigh vacuum conditions of our experiments, neither Ni(100) nor Pt(111) commonly exhibit C−C bond activation of alkyl fragments at temperatures low enough to compete with the hydrogenation and dehydrogenation that lead to hydrocarbon desorption. When temperatures high enough to cleave C−C bonds are reached, there is typically very little H available. Thus, a C_3 adsorbed species typically desorbs as a C_3 hydrocarbon or dehydrogenates and remains bound as carbon, at least up to 1200 K.

4.3. Comparison: C3 Adsorbates. For the purpose of comparing the thermal behavior of five C_3 adsorbates on Pt(111), Table 2 lists TPD products and peak temperatures. Briefly, the halogenated precursors lead to no halogenated hydrocarbon products. Iodine is removed as atomic I, whereas Cl (Br) desorbs as HCl (HBr). Strikingly, HCl is formed and desorbs at very low temperatures and, thus, provides an unusually low-temperature hydrogen removal route for ClC_3H_6I on Pt (111), with prior C−I bond breaking as a precondition.

Not surprisingly, propylene is a common product that, except for dosed C_3H_6, desorbs in multiple peaks between 185 and 325 K depending on the adsorbate. Multiple C_3H_6 desorption peaks is taken as evidence for multiple C_3H_x intermediates and multiple sources of H. For all five adsorbates, hydrogenation of η^3-allyl, $C_{(a)}H_2C_{(a)}HC_{(a)}H_2$, is proposed as the source of propylene at between 210 and 240 K. The lowest temperature propylene peaks (~185 K) are attributable to β-hydride elimination of *n*-propyl fragments. The 270 K C_3H_6 TPD peak from dosed C_3H_6 is generally attributed to thermally activated isomerization of di-σ-bonded C_3H_6.[31,33,34] In view of the results

SCHEME 1

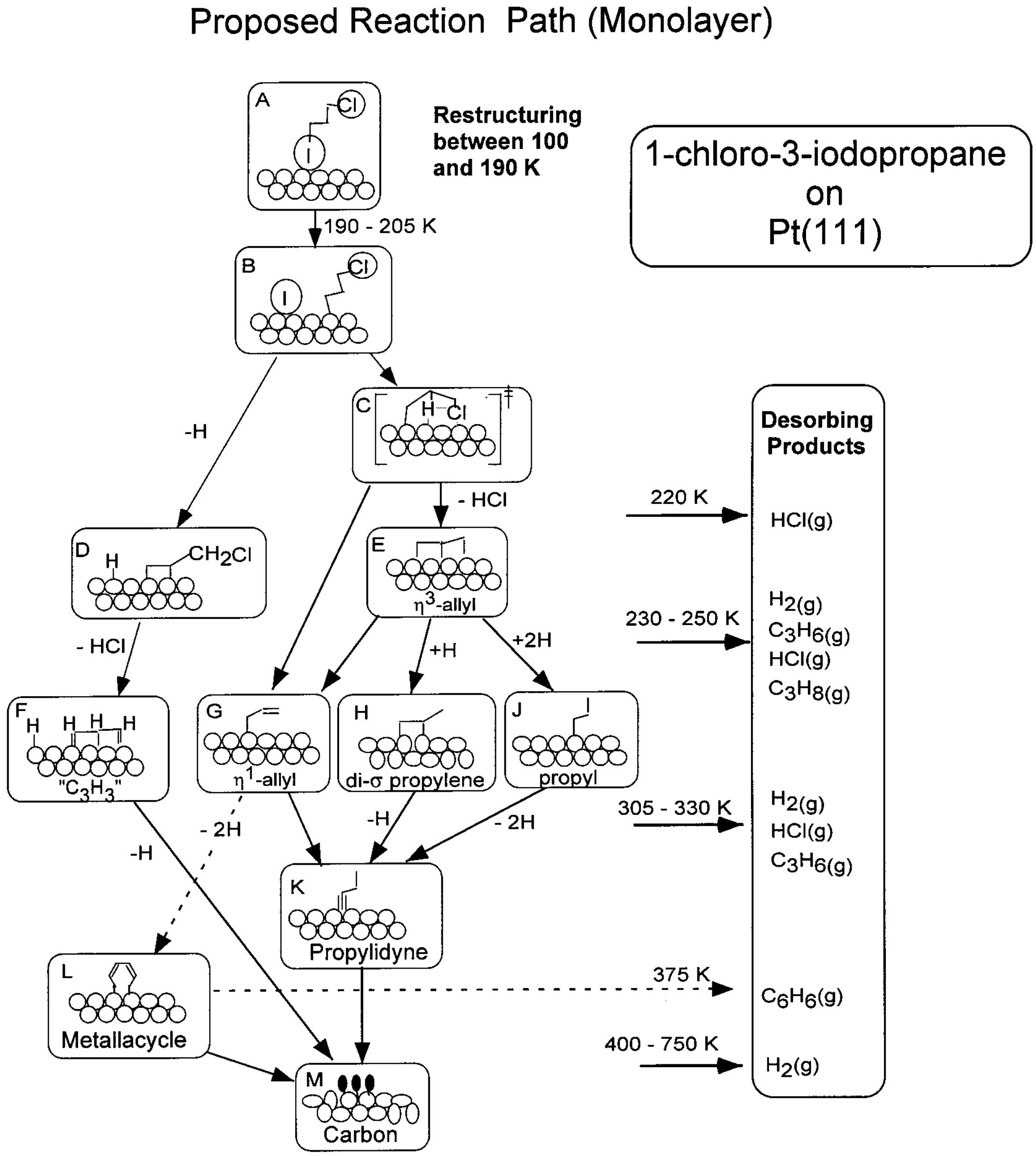

TABLE 2: TPD Products from C3 Adsorbates on Pt(111)

	product desorbing and peak temperature(s)							
adsorbate	H_2	HX	C_3H_6	C_3H_8	CH_4	C_2H_4	C_6H_6	halogen
ClC_3H_6I	250, 330, 430	220, 250, 305 (HCl)	240, 325	250	none	none	375	815 (I)
C_3H_7I[a]	260, 280, 325, 435	NA[e]	185, 240	240	none	none	none	825 (I)
C_3H_5Br[b]	280,325, 425	410 625 (HBr)	225, 320	225	none	none	none	none
C_3H_6[c]	300,325,425	NA	270	none	none	none	none	NA
c-C_3H_6[d]	315,430	NA	185, 210, 310	none	260	260	none	NA

[a] Reference 27. [b] Reference 26. [c] References 33 and 37.. [d] Electron irradiated.[1] [e] NA, not applicable.

for allyl bromide, C_3H_5Br,[24] we propose that η^1-allyl is an important intermediate leading to the evolution of C_3H_6 between 310 and 325 K.

It is noteworthy that propane, C_3H_8, is only found for halogenated C_3 adsorbates. This is the case even for the relatively H-deficient adsorbate, C_3H_5Br. We infer that the low temperature (~200 K) cleavage of C−X bonds leads to adsorbed C_3H_x fragments that differ from those formed either by electron irradiation of cyclopropane, c-C_3H_6,[1] or by adsorption of propylene. These differences lead to easily activated hydrogenation for the halogenated adsorbates.

Among the adsorbates, there are two unique observations. CH_4 and C_2H_4 are products only for electron irradiated c-C_3H_6.[1] Since they desorb coincidentally, we have assigned them to a common C_3 intermediate, namely, a metallocyclobutane. The other unique desorbing product is benzene found only for ClC_3H_6I. It is found only in very small amounts compared to, say, propylene and propane.

Finally, we give a more detailed discussion of the H_2 TPD results focusing on the four thermally activated C_3 adsorbates. Figure 10 compares H_2 TPD for monolayer coverages of iodopropane,[25] allyl bromide,[24] 1-chloro, 3-iodopropane, and

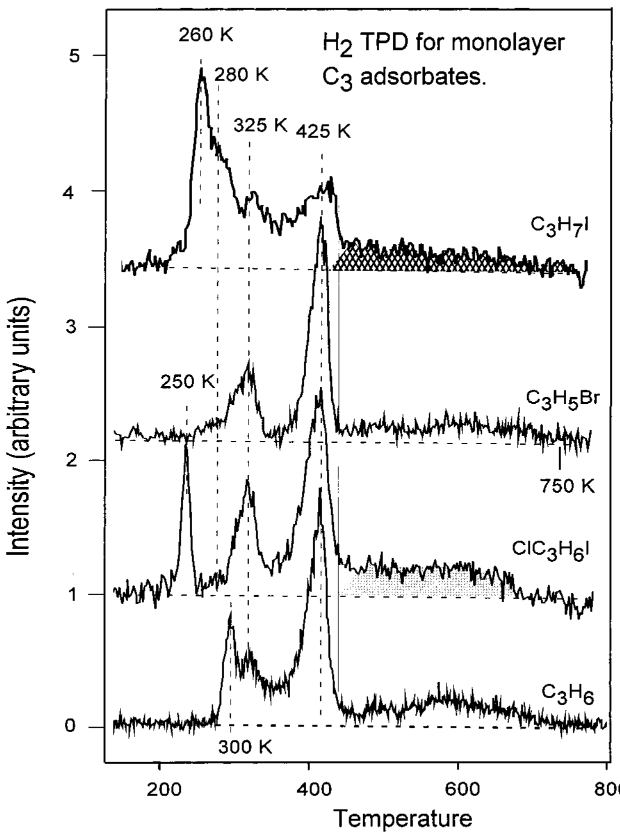

Figure 10. Comparison of H_2 TPD profiles for monolayer doses of C_3H_7I, C_3H_5Br, ClC_3H_6I, and C_3H_6 on Pt(111) at 100 K.

propylene.[31,35] The intensities of the four spectra are normalized to the height of the most intense peak, i.e., 425 K for three of the spectra and 260 K for iodopropane. For propylene, the peak at 425 K is well-established as arising from propylidyne dehydrogenation.[31,17] For both C_3H_5Br and ClC_3H_6I, there is clearly a sharp peak at 425 K, which we also attribute to propylidyne dehydrogenation. For C_3H_7I, the corresponding peak position is slightly higher, 435 K.

In all four cases, propylidyne, $C_{(a)}CH_2CH_3$, may be the only species dehydrogenating to give the 425 $\pm$ 10 K peak, but it is not the only C_xH_y species present between 350 and 400 K. For example, allyl and partially dehydrogenated allyl groups likely contribute in differing relative amounts. This is evidenced by the differing long, low intensity H_2 desorptions that extend to 750 K for propyl iodide, propylene, and allyl bromide and to 700 K for ClC_3H_6I. While the intensities between 450 and 750 K are relatively weak, there are reproducible differences, indicating that somewhat different C_xH_y distributions prevail in the three cases. The relatively low intensity of H_2 TPD above 450 K for C_3H_5Br is largely the result of HBr desorption which occurs throughout this regime.[24] There is a weak maximum around 575 K for C_3H_6 but not for the other three adsorbates. Furthermore, with respect to the peak in the 425−435 K region, the integrated relative intensities between 450 and 750 K are ordered (high to low) C_3H_7I (hatched area) > ClC_3H_6I (gray area) > C_3H_6 > C_3H_5Br. (Assuming, for the moment, that the peak at 435 K is due to propylidine dehydrogenation, the C_3H_7I profile must be multiplied by about 2.5 to bring the 435 K peak to the same height as the 425 K peaks of the three other spectra.) All of these observations point, not surprisingly, to other species mixed with propylidyne formed by heating the four adsorbates from 100 to 375 K.

Since, for C_3H_6, no hydrocarbons desorb, other than a small amount of C_3H_6 peaking at 280 K, and since the heating rate is linear, the average C_xH_y stoichiometery can be calculated at any temperature, T, by integration from 100 K to T, normalizing to the total H_2 TPD area, and multiplying by 6. This procedure gives C_3H_6 up to 275 K, $C_3H_{5.3}$ at 310 K, $C_3H_{4.3}$ at 350 K, $C_3H_{1.6}$ at 440 K. Thus, even for propylene, species other than propylidyne are present between 350 and 400 K.

In passing through the 250 K H_2 TPD peak for ClC_3H_6I, the C_xH_y stoichiometry drops from C_3H_6 to about $C_3H_{5.3}$ which takes account of both the H_2 and HCl desorptions. At 350 K, the C_xH_y stoichiometry drops to $C_3H_{3.8}$ based on complete desorption of Cl as HCl and 1.2 of the remaining five H's desorbed as H_2. At 450 K, the average C_xH_y stoichiometry is roughly $C_3H_{1.6}$ for C_3H_6, $C_3H_{1.8}$ for C_3H_5Br, and $C_3H_{1.4}$ for ClC_3H_6I.

Turning to the low-temperature region between 100 and 375 K, each adsorbate exhibits a distinct H_2 TPD intensity profile. In reverse thermal order, there are three common H_2 peaks or shoulders, 325, 300, and 280 K, for the halogenated adsorbates but only two peaks for C_3H_6, 325 and 300 K. In addition, there is a unique H_2 TPD peak at 260 K for C_3H_7I and at 250 K for ClC_3H_6I.

Interestingly, for the adsorbate, C_3H_7I, with the highest initial H/C ratio, 7:3, the H_2 distribution peaks at low temperature (260 K), just after a major propane desorption peak and a somewhat smaller propylene desorption peak.[25] There are two attractive reaction paths leading to these products. First, β-hydride elimination of propyl groups to form propylene and atomic hydrogen. The latter could hydrogenate neighboring propyl to propane that desorbs, while the former could follow two paths: desorption as propylene and retention as di-σ-bonded propylene. A second possible reaction leading to these products is disproportionation of propyl groups to form desorbing propane and propylene along with some di-σ-bonded propylene, i.e., $2C_{(a)}H_2CH_2CH_3 \rightarrow C_3H_8(g) + C_3H_6(g)$ or $C_{(a)}H_2C_{(a)}HCH_3$. It is significant that this path does not form surface bound H. Along either of the two proposed paths, as the temperature rises, $C_{(a)}H_2C_{(a)}HCH_3$ undergoes dehydrogenation to propylidyne, accounting for a significant portion of the 300 and 325 K peaks.

It is of interest to consider C_3H_5Br in more detail because, among the four adsorbates, it has the lowest initial H/C ratio, 1.67. For the conditions of Figure 10, some propane desorbs at 225 K and a relatively large amount of propylene desorbs at 320 K. The propylene desorption tracks the H_2 TPD between 276 and 375 K. Desorption of these and H_2 reduces the H/C ratio, and thus, the average stoichiometry at 375 K is well below 1.67, the C/H ratio in propylidyne. Nevertheless, the presence and dehydrogenation of propylidyne is indicated by the strong H_2 TPD peak at 425 K. By correlation with the results for propylene, the formation of propylidyne during C_3H_5Br TPD is suggested by the H_2 TPD peak at 325 K. If so, there must be multiple active hydrogenation and dehydrogenation paths involving η^3-allyl, $C_{(a)}H_2C_{(a)}HC(a)H_2$, the product formed by heating C_3H_5Br.[24] The only source of hydrogen is C−H bonds, and the clear implication is that there are C_xH_y species other than propylidyne at 375 K in the TPD of C_3H_5Br. Evidently, C−H bond breaking sets in at 225 K, but only in certain crowded locations, where it is promptly consumed by $C_{(a)}H_2C_{(a)}HC(a)H_2$ in two steps to form propane that desorbs promptly. In the same temperature region, propane desorbs in the TPD of propyl iodide.[25] We propose that, as the temperature exceeds 250 K, the rates of hydrogenation and dehydrogenation accelerate, and there is a narrow temperature interval where the local concentrations of $H_{(a)}$ and $C_{(a)}H_2C_{(a)}HC(a)H_2$ are both transiently high enough to form adsorbed C_3H_6, which either desorbs, if neighboring Pt atoms are occupied, or forms di-σ-bonded propylene if neighboring Pt atoms are available. In this process, adsorbed $C_3H_{y<5}$ species are also formed.

The very narrow H_2 TPD peak at 250 K, with an onset at 225 K, for the ClC_3H_6I spectrum is unique but clearly suggests that, as for C_3H_7I, easily detectable C−H bond breaking in C_3 adsorbates sets in as low as 225 K on Pt(111) when certain conditions are met. As for C_3H_7I,[25] there is also a strong low-temperature propane peak indicating that hydrogenation processes compete successfully with dehydrogenation processes even though the H/C ratio in the adsorbate is low. The latter implies that significant concentrations of active hydrogen must be available at relatively low temperatures. The consumption of available H by these routes, and by HCl desorption, certainly reduces the average H/C ratio in the species at 375 K to a value well below that characterizing C_3H_6 TPD. There is also C_3H_8 desorption at 250 ± 10 K for C_3H_5Br TPD, so the initial H/C ratio is not critical. Rather, we presume the local coverage is crucial and that η^3-allyl is thermodynamically favored but its formation requires availability of neighboring Pt sites. Availability depends, to some extent, on the adsorbate and is probably highest for C_3H_5Br where the adsorption into a nondissociative state at 100 K places the principal axis of the molecule roughly parallel to the surface and where the C−Br bond breaking forms η^3-allyl directly.[24]

Using this local coverage model, the unique low-temperature H_2 and C_3H_8 TPD (250 K) peaks observed during ClC_3H_6I TPD can be rationalized in the following way. On a local basis for ClC_3H_6I, Pt site availability will increase during TPD if C_3 moieties desorb and will decrease if C−H and C−X bond breaking occurs leading to adsorbed C_3 species with multiple C atoms bound to Pt. In any local region where the initial coverage reaches or exceeds a critical value, perhaps ML, the cleavage of C−I bonds between 160 and 220 K, as typical for iodides, will lead to a dense array of I(a) and $C_{(a)}H_2CH_2CH_2Cl$ strongly bound to Pt with few, if any, neighboring unoccupied Pt sites. As the temperature rises into a thermal region where C−H and C−Cl bonds become activated, it is difficult for the nascent Cl or H to access an available Pt site. This inhibits chemisorption and makes desorption competitive. One plausible desorption route is concerted formation of HCl and H_2 through intra- or interadsorbate coupling. A second, nonconcerted desorption route involves C−Cl or C−H bond cleavage followed by prompt abstraction of H or Cl from a neighboring fragment. A third route for H atoms is hydrogenation of C_3H_6 to form C_3H_7 that, because of local congestion, finds dehydrogenation inhibited and hydrogenation to propane competitive. As these products desorb, Pt sites become available and, in our model, species such as η^3-allyl form in the presence of $I_{(a)}$ and $C_3H_{x<5}$.

5. Summary

The thermal chemistry of ClC_3H_6I adsorbed on Pt(111) has been followed using TPD, XPS, and HREELS. The results indicate that for ClC_3H_6I in contact with Pt, the C−I dissociation occurs during heating, the onset temperature increasing and dissociation probability decreasing with initial coverage. The vibrational spectra change significantly even before C−I bond breaking, indicating restructuring of the adsorbed layer. The undissociated fraction desorbs molecularly above 200 K. Once the C−I bond breaks, the resulting chloropropyl fragment exhibits a low-temperature reaction path that desorbs HCl and leaves η^3-allyl, a key intermediate species that follows multiple paths depending on the local environment and the availability of active atomic hydrogen. These paths lead to *n*-propyl, di-σ-bonded propylene, and isomerization to η^1-allyl. The chloropropyl fragment also dehydrogenates to supply some surface hydrogen and the resulting di-σ-bonded chloropropylene species loses HCl to desorption. The resulting H-deficient C_3H_3 moiety is proposed as an additional source of surface H atoms that, along with η^3-allyl, supplies H for formation of propylene and propane. The η^3-allyl that dehydrogenates forms propylidyne. There is a small amount of benzene desorption attributed to linking, with H loss, of a pair of η^1-allyl species.

Acknowledgment. This work was supported in part by the U. S. Department of Energy, Office of Basic Energy Sciences, and by the Robert A. Welch Foundation. T.B.S. thanks E. D. Pylant and K. H. Junker for their helpful discussions.

References and Notes

(1) Scoggins, T. B.; Ihm, H.; Sun, Y.-M.; White, J. M. *J. Phys. Chem.*, submitted.
(2) Anderson, J. R.; Avery, N. R. *J. Catalysis* **1967**, *8*, 48.
(3) Madey, T. E.; Yates, J. T. *Surf. Sci.* **1978**, *76*, 397.
(4) Hoffman, F. M.; Felter, T. E.; Weinberg, W. H. *J. Chem. Phys.* **1982**, *76*, 3799.
(5) Felter, T. E.; Hubbard, A. T. *J. Electroanalytical Chem.* **1979**, *100*, 473.
(6) Franz, A. J.; Ranney, J. T.; Gland, J. L.; Bare, S. R. *Surf. Sci.* **1997**, *374*, 162.
(7) Martel, R.; Rochefort, A.; McBreen, P. H. *J. Am. Chem. Soc.* **1994**, *116*, 5965.
(8) Martel, R.; Rochefort, A.; McBreen, P. H. *J. Am. Chem. Soc.* **1998**, *120*, 2421−2427.
(9) Engstrom, J. R.; Goodman, D. W.; Weinberg, W. H. *J. Phys. Chem.* **1990**, *94*, 396.
(10) Kelly, D.; Weinberg, W. H. *J. Chem. Phys.* **1996**, *105*, 7171.
(11) Jachimowski, T. A.; Weinberg, W. H. *Surf. Sci.* **1997**, *370*, 71.
(12) Brown, R.; Kemball, C. J. *J. Chem. Soc., Faraday Trans.* **1990**, *86*, 3815.
(13) Wallace, H. F.; Hayes, K. E. *J. Catal.* **1973**, *29*, 83.
(14) Schwank, J.; Lee, Y.; Goodwin, J. G. *J. Catal.* **1987**, *108*, 495.
(15) Kahn, D. R.; Petersen, E. E.; Somorjai, G. A. *J. Catal.* **1974**, *34*, 294.
(16) Lenz-Solomun, P.; Goodman, D. W. *Langmuir* **1994**, *10*, 172.
(17) Addy, J.; Bond, G. C. *Trans. Faraday Soc.* **1957**, *53*, 368.
(18) Sridhar, T. S.; Ruthven, D. M. *J. Catal.* **1972**, *24*, 153.
(19) Bent, B. E.; Nuzzo, R. G.; Zegarski, B. R.; DuBois, L. H. *J. Am. Chem.* **1991**, *113*, 1137.
(20) Subscript “(a)” denotes atom bound to Pt.
(21) Zhou, X.-L.; White, J. M. *J. Vac. Sci. Technol. A* **1993**, *11*, 2210.
(22) Tjandra, S.; Zaera, F. *J. Am. Chem. Soc.* **1995**, *117*, 9749.
(23) Tjandra, S.; Zaera, F. *J. Phys. Chem. B* **1997**, *101*, 1006−1013.
(24) Scoggins, T. B.; White, J. M. *J. Phys. Chem.* **1997**, *101*, 7958−67.
(25) Scoggins, T. B.; Ihm, H.; White, J. M. *Isr. J. Chem.* **1998**, *38*, 353−363.
(26) Norton, P. R.; Davies, J. A.; Jackman, T. E. *Surf. Sci.* **1982**, *122*, L593.
(27) Zaera, F. *Surf. Sci.* **1989**, *219*, 453.
(28) Liu, Z.-M.; Zhou, X.-L.; Buchanan, D. A.; Kiss, J.; White, J. M. *J. Am. Chem. Soc.* **1992**, *114*, 2031.
(29) Jo, S. K.; White, J. M. *Surf. Sci.* **1992**, *261*, 111.
(30) Thorbjornsrud, J.; Ellestad, O. H.; Klaboe, P.; Torgrimsen, T. *J. Mol. Struct.* **1973**, *15*, 61.
(31) Ogle, K. M.; Creighton, J. R.; White, J. M. *Surf. Sci.* **1986**, *169*, 246.
(32) Zhou, X.-L.; White, J. M. *J. Am. Chem. Soc.* **1991**, *95*, 5575−5580.
(33) Avery, N. R.; Sheppard, N. *Proc. R. Soc. London A* **1986**, *405*, 1.
(34) Koestner, R. J.; Hove, M. A. V.; Somorjai, G. A. *J. Phys. Chem.* **1983**, *87*, 203.
(35) Scoggins, T. B. Surface Chemistry of C_3 Hydrocarbons on Platinum. University of Texas, 1997.